

---

# Adversarial Shapley Value Experience Replay for Task-Free Continual Learning

---

**Dongsub Shim** \*  
University of Toronto  
dongsub.shim@mail.utoronto.ca

**Zheda Mai** \*  
University of Toronto  
zheda.mai@mail.utoronto.ca

**Jihwan Jeong** \*  
University of Toronto  
jhjeong@mie.utoronto.ca

**Scott Sanner**  
University of Toronto  
ssanner@mie.utoronto.ca

**Hyunwoo Kim**  
LG Sciencepark  
eugenehw.kim@lgsp.co.kr

**Jongseong Jang**  
LG Sciencepark  
j.jang@lgsp.co.kr

## Abstract

Continual learning is a branch of deep learning that seeks to strike a balance between learning stability and plasticity. In this paper, we specifically focus on the task-free setting where data are streamed online without task metadata and clear task boundaries. A simple and highly effective algorithm class for this setting is known as Experience Replay (ER) that selectively stores data samples from previous experience and leverages them to interleave memory-based and online batch learning updates. Recent advances in ER have proposed novel methods for scoring which samples to store in memory and which memory samples to interleave with online data during learning updates. In this paper, we contribute a novel Adversarial Shapley value ER (ASER) method that scores memory data samples according to their ability to preserve latent decision boundaries for previously observed classes (to maintain learning stability and avoid forgetting) while interfering with latent decision boundaries of current classes being learned (to encourage plasticity and optimal learning of new class boundaries). Overall, we observe that ASER provides competitive or improved performance on a variety of datasets compared to state-of-the-art ER-based continual learning methods.

## 1 Introduction

Humans confront new information throughout their lifespan and have the ability to learn, refine, and transfer knowledge and skills continually. However, without special techniques, neural networks cannot easily learn in this manner due to *catastrophic forgetting* [23] – the inability of a network to perform well in previously seen tasks after learning new tasks. For this reason, conventional deep learning tends to focus on offline training, where each mini-batch is sampled iid from a static dataset with multiple epochs over the training data. Continual Learning (CL) studies the problem of learning from a non-iid stream of data, with the goal of preserving and extending the acquired knowledge.

Many existing CL approaches use a *known task* incremental setting where data arrives one task at a time and the model can utilize task metadata during both training and testing [14, 19, 20]. However,

---

\* Authors contributed equally

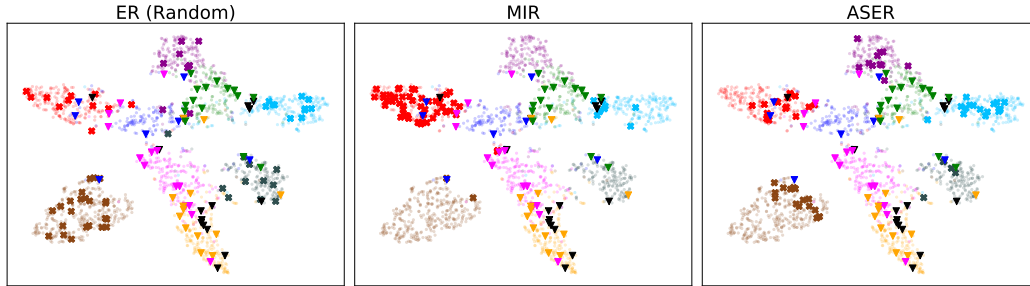


Figure 1: 2D t-SNE [21] visualization of CIFAR-100 data embeddings and their class labels (different colors) showing current task samples (triangle), memory samples (pale circle) and retrieved memory samples for rehearsal (bold x). For each point, we obtain the latent embedding from reduced ResNet18 [5]. Note that ER (Random) distributes its retrieved samples non-strategically, MIR disproportionately selects seemingly redundant samples in a single – apparently most interfered – class (red), whereas ASER strategically retrieves memory samples that are representative of different classes in memory but also adversarially located near class boundaries and current task samples.

a more realistic setting is known as *task-free* CL, where data are streamed online (each sample is seen only once) without task metadata and clear task delineation [2, 9]. This practical task-free setting has received much attention recently [1, 3, 2, 16] and is the setting we focus on in this paper.

Current CL methods can be taxonomized into three major categories: prior-focused, parameter isolation, and memory-based methods [26, 7]. Prior-focused methods encode the knowledge from past tasks into a prior and utilize the prior to either regularize the update of parameters that were important to past tasks [14, 34] or penalize the feature drift on previous tasks [19, 25]. Parameter isolation methods assign per-task parameters to bypass interference by expanding the network and masking parameters to prevent forgetting [22, 16, 33]. Memory-based methods use a memory buffer to store a subset of data from previous tasks. The samples from the buffer can be either used to constrain the parameter updates such that the loss on previous tasks cannot increase [5, 20], or simply for replay to prevent forgetting [6]. In this work, we consider the replay approach since it has shown to be successful and efficient for the task-free setting [3, 1], with the key questions being *how to update and retrieve memory samples when new data arrives?* For example, Experience Replay (ER) [6] randomly selects samples, while the highly effective Maximally Interfered Retrieval (MIR) method [1] chooses replay samples whose loss most increases after a current task update. However, if we visualize the latent space of retrieved memory samples chosen by each method in Figure 1, we see that ER and MIR fail to strategically select samples that both preserve existing memory-based class boundaries while protecting against current task samples that interfere with these boundaries.

We address the deficiencies observed above by proposing a novel replay-based method called Adversarial Shapley value Experience Replay (ASER). ASER is inspired by the Shapley value (SV) [30] used in cooperative game theory to fairly distribute total gains to all players — in our CL setting, we use the SV to determine the contribution of memory samples to learning performance [11, 12, 13]. We also introduce an adversarial perspective of SV for CL memory retrieval that aims to score memory samples according to their preservation of decision boundaries for “friendly” samples in the memory buffer (to maintain learning stability and avoid forgetting) and their interference with “opponent” samples from the current task that disrupt existing memory-based class boundaries (to encourage plasticity and optimal learning). Through extensive experiments on three commonly used benchmarks in the CL literature, we demonstrate that ASER provides competitive or improved performance compared to state-of-the-art replay-based methods as well as various ablations of ASER.

## 2 Continual Learning

### 2.1 Problem Definition

**Task-Free CL** We consider the task-free CL setting for the supervised learning problem with an online (potentially infinite) stream of data, following the recent CL literature [1, 3, 16]. More concretely, a neural network classifier  $f : \mathbb{R}^d \mapsto \mathbb{R}^C$ , parameterized by  $\theta$  will receive input batches

$B_n$  of size  $b$  that are drawn non-iid from a current distribution  $D_t$  at task  $t$ . Note the distribution  $D_t$  could change suddenly or gradually and the classifier has no access to any of the task metadata during training and testing. Our goal is to train the classifier  $f$  to continually learn new samples from the data stream without interfering with the performance of previously observed samples.

**Metrics** Since the goal of CL is to continually acquire new knowledge while preserving existing learning, we use two standard metrics in the CL literature to measure performance: average accuracy for overall performance and forgetting to measure how much acquired knowledge the algorithm has forgotten [4, 6]. In **Average Accuracy**,  $a_{i,j}$  is the accuracy evaluated on the held-out test set of task  $j$  after training the network from task 1 to  $i$ . In **Average Forgetting**,  $f_{i,j}$  represents how much the model forgets about task  $j$  after being trained on task  $i$ . There are  $T$  total tasks.

$$\text{Average Accuracy}(A_T) = \frac{1}{T} \sum_{j=1}^T a_{T,j} \quad \text{Average Forgetting}(F_T) = \frac{1}{T-1} \sum_{j=1}^{T-1} f_{T,j}$$

$$\text{where } f_{i,j} = \max_{l \in \{1, \dots, i-1\}} a_{l,j} - a_{i,j}$$

## 2.2 Experience Replay Methods

**Experience Replay (ER)** The research of ER and the important role of replay buffers has been well-established in the reinforcement learning area [28, 10]. Recently, ER has been widely applied in supervised CL learning tasks [27, 1, 3]. Compared with the simplest baseline model that fine-tunes the parameters based on the new task without any measures to prevent forgetting, ER makes two simple modifications: (1) it stores a subset of the samples from past tasks in a memory buffer  $\mathcal{M}$  of limited size  $M$ ; (2) it concatenates the incoming minibatch  $B_n$  with another minibatch  $B_{\mathcal{M}}$  of samples selected from the memory buffer. Then, it simply takes a SGD step with the combined batch, followed by an online update of the memory. A generic ER algorithm is presented in Algorithm 1.

What differentiates various replay-based methods are the *MemoryRetrieval* in line 3 and the *MemoryUpdate* in line 5. Although there exists another stream of replay methods that utilize a generative model to produce virtual samples instead of using a memory buffer [31], recent research has demonstrated the limitations of such approaches with convolutional neural networks in datasets such as CIFAR-10 [1, 17]. Hence, we focus on the memory-based approach in our work.

Basic **ER** is a simple but strong baseline that applies reservoir sampling in *MemoryUpdate* and random sampling in *MemoryRetrieval*. Despite its simplicity, recent research has shown that naive ER outperforms many specifically designed CL approaches with and without a memory buffer [6].

---

### Algorithm 1: Generic ER-based method

---

**Input** : Batch size  $b$ , Learning rate  $\alpha$   
**Initialize:** Memory  $\mathcal{M} \leftarrow \{\} * M$ ;  
Parameters  $\theta$ ; Counter  $n \leftarrow 0$

- 1 **for**  $t \in \{1, \dots, T\}$  **do**
- 2     **for**  $B_n \sim D_t$  **do**
- 3          $B_{\mathcal{M}} \leftarrow \text{MemoryRetrieval}(B_n, \mathcal{M})$
- 4          $\theta \leftarrow \text{SGD}(B_n \cup B_{\mathcal{M}}, \theta, \alpha)$
- 5          $\mathcal{M} \leftarrow \text{MemoryUpdate}(B_n, \mathcal{M})$
- 6          $n \leftarrow n + b$
- 7 **return**  $\theta$

---

### Maximally-interfered Retrieval (MIR)

MIR is a recently proposed method aiming to improve the *MemoryRetrieval* strategy [1]. MIR chooses replay samples according to loss increases given the estimated parameters update based on the newly arrived data. However, samples with significant loss increases tend to be similar in the latent space, which may lead to redundancy in the retrieved data, as shown in Figure 1. Like ER, MIE uses reservoir sampling for the *MemoryUpdate*.

### Gradient-based Sample Selection (GSS)

Different from MIR, GSS pays attention to the *MemoryUpdate* strategy [3]. Specifically, it tries to diversify the gradients of the samples in the memory buffer. Like ER, GSS uses random sampling in *MemoryRetrieval*.

### 3 Efficient Computation of Shapley Value via KNN Classifier

When we return to Figure 1 and analyze the latent embeddings of memory samples, we observe the natural clustering effect of classes in the embedding space, which has been well-observed previously in the deep learning literature [24, 8]. On account of this, we observe that some samples may indeed be more important than others in terms of preserving what the neural network has learned. For example, data from one class that are near the boundary with data from another class in some sense act as sentinels to guard the decision boundary between classes. This suggests the following question: *how can we value data in the embedded space in terms of their contribution to accurate classification?*

Given that the embedding plot of Figure 1 suggests that a new data point is likely to take the classification of its nearest neighbors in the embedding space, we could rephrase this question as asking how much each data point in memory contributes to correct classification from the perspective of a K-Nearest Neighbors (KNN) classifier. Fortunately, the existing research literature already provides both a precise and efficient answer to this question viewed through the lens of Shapley data valuation for KNN classifiers [12, 11, 13]. Before we cover this solution, we first pause to recap the purpose of Shapley values.

**Shapley Value (SV) for Machine Learning** The SV [30, 29] was originally proposed in cooperative game theory to decide the share of total gains for each player in a coalition. The SV has a set of mathematical properties that make it appealing to many applications: *group rationality*, *fairness*, and *additivity*. Conversely, it can be shown that the SV is the *only* allocation scheme that satisfies these three properties.

In the context of machine learning, the SV has been used to estimate the individual contribution of data points to the performance of a trained model *in the context of all other data* [11, 13]. Formally, let  $N$  denote the number of data points and  $I = \{1, \dots, N\}$  be the associated index set. Then, each datum is interpreted as a player of a cooperative game with the goal of maximizing test-time performance. Let  $v(S)$  define a utility function of the ML model over a subset  $S \subset I$  on which the model is trained. Then, the SV of a data point of index  $i$  with the utility  $v(S)$  is the following:

$$s(i) = \frac{1}{N} \sum_{S \subseteq I \setminus \{i\}} \frac{1}{\binom{N-1}{|S|}} [v(S \cup \{i\}) - v(S)] \quad (1)$$

Intuitively, when we consider every possible subset of data points,  $s(i)$  measures the average marginal improvement of utility given by the sample  $i$ . By setting the utility as test accuracy in ML classification tasks, the SV can discover how much of the test accuracy is attributed to a training instance.

**Efficient KNN Shapley Value Computation** Specific to our requirements for data valuation in this paper, recent work has developed an efficient method for SV computation in a KNN classification framework [12]. This is a critical innovation since the direct powerset-based computation of the SV requires  $O(2^N)$  evaluations for general, bounded utility functions. Furthermore, each evaluation involves training an ML model with a given subset of data ( $S$ ). This is prohibitive in most modern deep learning applications, not to mention online CL with neural networks. As shown in [12] and summarized below, the exact KNN-SV can be computed in  $O(N \log N)$ .

Let  $(\mathbf{x}_j^{\text{ev}}, y_j^{\text{ev}})$  denote an *evaluation point* and  $D_c = \{(\mathbf{x}_i, y_i)\}_{i=1}^{N_c}$  a *candidate set*. We compute the KNN-SVs of all examples in  $D_c$  w.r.t. the evaluation point with the utility function (2). The KNN utility function over a subset  $S \subset D_c$  measures the likelihood of correct classifications:

$$v_{j,\text{KNN}}(S) = \frac{1}{K} \sum_{k=1}^{\min(K, |S|)} \mathbb{1}[y_{\alpha_k(S)} = y_j^{\text{ev}}] \quad (2)$$

where  $\alpha_k(S)$  is the index of the  $k$ th closest sample (from  $\mathbf{x}_j^{\text{ev}}$ ) in  $S$ . Each sample  $i$  is assigned a KNN-SV —  $s_j(i)$  — that represents the average marginal contribution of the instance to the utility. Due to the additivity of SV, we obtain the KNN-SV of a candidate sample w.r.t. the evaluation set ( $D_e = \{(\mathbf{x}_j^{\text{ev}}, y_j^{\text{ev}})\}_{j=1}^{N_e}$ ) by taking the average:  $s_{\text{avg}}(i) = 1/N_e \sum_{j=1}^{N_e} s_j(i)$ .

(3) and (4) show how to recursively compute the exact KNN-SVs of samples in  $D_c$  w.r.t.  $(\mathbf{x}_j^{\text{ev}}, y_j^{\text{ev}}) \in D_e$  starting from  $\mathbf{x}_{\alpha_{N_c}}$  (the farthest point from  $\mathbf{x}_j^{\text{ev}}$ ) [12]:

$$s_j(\alpha_{N_c}) = \frac{\mathbb{1}[y_{\alpha_{N_c}} = y_j^{\text{ev}}]}{N_c} \quad (3)$$

$$s_j(\alpha_m) = s_j(\alpha_{m+1}) + \frac{\mathbb{1}[y_{\alpha_m} = y_j^{\text{ev}}] - \mathbb{1}[y_{\alpha_{m+1}} = y_j^{\text{ev}}]}{K} \frac{\min(K, m)}{m} \quad (4)$$

Here,  $s_j(\alpha_m)$  is the KNN-SV of the  $m$ th closest candidate sample from  $\mathbf{x}_j^{\text{ev}}$ . Note that the dependency on the utility  $v$  is suppressed as  $v_{\text{KNN}}$  is always used. We refer readers to [12] for detailed derivation of these results.

## 4 Adversarial Shapley Value Experience Replay (ASER)

We have now affirmatively answered how to value data in the embedded space in terms of its contribution to accurate classification by leveraging the efficient KNN SV computation. Equipped with this powerful global data valuation algorithm, we now present our novel ER method dubbed Adversarial Shapley value ER (ASER) that leverages the SV for both *MemoryRetrieval* and *MemoryUpdate*.

A key insight with our ASER approach for *MemoryRetrieval* is that we need to balance the competing needs at the crux of CL, i.e., we need to retrieve memory samples for replay that prevent forgetting while also finding samples that maximally interfere with the incoming batch  $B_n$  to ensure plasticity in learning. This leads us not only to leverage a cooperative notion of the SV (where higher SV is better) as it relates to  $\mathcal{M}$  but also an adversarial notion of the SV as it relates to  $B_n$  (where lower – and, in fact, negative – SVs indicate interference). In addition ASER also adopts a cooperative SV approach to the *MemoryUpdate* process.

Formally, we can view a neural network classifier ( $f$ ) as two separate parts: a feature extractor ( $f_{\text{ext}} : \mathbb{R}^d \mapsto \mathbb{R}^h$ ) and a fully connected neural classifier ( $f_{\text{cl}} : \mathbb{R}^h \mapsto \mathbb{R}^C$ ), where  $h$  is the dimensionality of the latent space  $\mathcal{X}^l$ . We implicitly define a KNN classifier and use the Euclidean distance in  $\mathcal{X}^l$ . Then, by (3)-(4), we can compute the KNN-SVs of candidate samples w.r.t. evaluation samples.

As previously noted, ER’s performance depends on deciding what to store in memory (i.e., *MemoryUpdate*) and what to replay from memory (i.e., *MemoryRetrieval*). One key desiderata is that we want samples in  $\mathcal{M}$  as well as  $B_n$  to be well-separated by  $f_{\text{ext}}$  in the latent space. To this end, we target two types of samples in  $\mathcal{M}$  for retrieval: those near the samples in  $B_n$  but have different labels (Type 1); those that are representative of samples in the memory (Type 2). Training with samples in Type 1 encourages the model to learn to differentiate current classes from previously seen classes. Samples in Type 2 help retain latent decision boundaries for previously observed classes.

We ground our intuition as to how samples interfere and cluster with each other in the latent space based on two properties of the KNN-SV. Given a candidate sample  $i \in D_c$  and an evaluation set  $D_e$ , the KNN-SV of the point  $i$  w.r.t. an evaluation point  $j \in D_e$ , i.e.  $s_j(i)$ , satisfies the following (see Appendix B for proof):

Property 1.  $s_j(i) > 0$  if  $y_i = y_j^{\text{ev}}$  and  $s_j(i) \leq 0$  if  $y_i \neq y_j^{\text{ev}}$ . The equality holds if and only if  $S = \{i' | y_{i'} = y_j^{\text{ev}}, \forall i' \in \{1, \dots, N_c\}\} = \emptyset$ .

Property 2.  $|s_j(\alpha_m)|$  is a non-increasing function of  $m$  where  $\alpha_m$  is the  $m$ th closest point in  $D_c$  from  $j$  in the latent space. And for  $m \geq K$ ,  $|s_j(\alpha_m)| - |s_j(\alpha_{m+1})| > 0$  if  $y_{\alpha_m} \neq y_{\alpha_{m+1}}$ . In other words,  $|s_j(i)|$  cannot decrease as  $i$  gets closer to the evaluation point  $j$ , and it can only increase when the label changes for  $m \geq K$ .

The first property states that a candidate sample  $i$  has a *positive KNN-SV* if it has the same label as the evaluation point being considered (*cooperative*); the sample will have a *negative KNN-SV* if its label is different than the evaluation point (*adversarial*). By combining both properties, we note:

If  $s_j(i)$  is large, the candidate  $i$  is close to the evaluation point  $j$  in the latent space ( $\mathcal{X}^l$ ) and has the same label ( $y_i = y_j^{\text{ev}}$ ). On the other hand, if  $s_j(i)$  is a negative value of large magnitude, then  $i$  is close to  $j$ , yet has a different label ( $y_i \neq y_j^{\text{ev}}$ ). Thus, we conjecture that a good data candidate  $i$  has *high positive SV* for memory  $\mathcal{M}$  and *low negative SV* for the current input task  $B_n$ .

When we consider the whole evaluation set, we take the mean  $s_{D_e}(i) = 1/|D_e| \cdot \sum_{j \in D_e} s_j(i)$ , and the above analysis still holds in average. Therefore, by examining the KNN-SVs of candidate samples,

we can get a sense of how they are distributed with respect to the evaluation set in  $\mathcal{X}^l$ . Then, we define the **adversarial SV (ASV)** that encodes the Type 1 & 2 criteria

$$\mathbf{ASV}(i) = \max_{j \in S_{\text{sub}}} s_j(i) - \min_{k \in B_n} s_k(i), \quad \forall i \in \mathcal{M} \setminus S_{\text{sub}}, \quad (5)$$

as well as a ‘‘softer’’ mean variation  $\mathbf{ASV}_\mu$

$$\mathbf{ASV}_\mu(i) = \frac{1}{|S_{\text{sub}}|} \sum_{j \in S_{\text{sub}}} s_j(i) - \frac{1}{b} \sum_{k \in B_n} s_k(i), \quad \forall i \in \mathcal{M} \setminus S_{\text{sub}}, \quad (6)$$

where  $S_{\text{sub}}$  is constructed by subsampling some number of examples from  $\mathcal{M}$  such that it is balanced in terms of the number of examples from each class. This prevents us from omitting any latent decision boundaries of classes in the memory. Note that  $S_{\text{sub}}$  is used as the evaluation set in the first term, whereas the input batch  $B_n$  forms the evaluation set in the latter term. The candidate set is  $\bar{\mathcal{M}} = \mathcal{M} \setminus S_{\text{sub}}$ , and we retrieve samples of size  $b_{\mathcal{M}}$  from the set that have the highest  $\mathbf{ASV}$ s (Algorithm 2). We denote our ER method using the score  $\mathbf{ASV}$  (5) as ASER, while  $\text{ASER}_\mu$  uses  $\mathbf{ASV}_\mu$  (6) instead. For computational efficiency, we randomly subsample  $N_c$  candidates from  $\bar{\mathcal{M}}$ .

---

**Algorithm 2: ASER MemoryRetrieval**

---

**Input** : Memory batch size  $b_{\mathcal{M}}$   
Input batch  $B_n$ ; Candidate size  $N_c$ ;  
Subsample size  $N_{\text{sub}}$ ;  
Feature extractor  $f_{\text{ext}}$

- 1  $S_{\text{sub}} \stackrel{N_{\text{sub}}}{\sim} \mathcal{M}$  // get evaluation set
- 2  $D_c \stackrel{N_c}{\sim} \mathcal{M} \setminus S_{\text{sub}}$  // get candidate set
- 3 /\* get latent embeddings \*/  
 $L_{B_n}, L_{S_{\text{sub}}}, L_{D_c} \leftarrow f_{\text{ext}}(B_n), f_{\text{ext}}(S_{\text{sub}}), f_{\text{ext}}(D_c)$
- 4 **for**  $i \in D_c$  **do**
- 5     **for**  $j \in S_{\text{sub}}$  **do**
- 6          $s_j(i) \leftarrow \text{KNN-SV}(L_{D_c}, L_{S_{\text{sub}}})$  as per (3), (4)
- 7     **for**  $k \in B_n$  **do**
- 8          $s_k(i) \leftarrow \text{KNN-SV}(L_{D_c}, L_{B_n})$  as per (3), (4)
- 9      $score(i) \leftarrow \mathbf{ASV}(i)$  as per (5) or (6)
- 10  $B_{\mathcal{M}} \leftarrow b_{\mathcal{M}}$  samples with largest  $score(\cdot)$
- 11 **return**  $B_{\mathcal{M}}$

---

Note that both ASER methods do not greedily retrieve samples with the smallest distances to either  $S_{\text{sub}}$  or  $B_n$ . This is because for a single evaluation point  $j$ ,  $s_j(\alpha_m) = s_j(\alpha_{m+1})$  when  $y_{\alpha_m} = y_{\alpha_{m+1}}$ . So, a few points can have the same score even if some of them are farther from the evaluation point. This is in contrast to a pure distance-based score where the closest point gets the highest score. In Appendix D, we show that our method outperforms pure distance-based methods, proving the effectiveness of the global way in which the SV scores candidate data based on the KNN perspective.

We summarize our method in Algorithm 2, and compare it with other state-of-the-art ER methods on multiple challenging CL

benchmarks in Section 5.

**Memory Update Based on KNN-SV** For *MemoryUpdate*, we find that samples with high KNN-SV are useful to store in the memory, which aligns with the original meaning of the SV. More concretely, we subsample  $S_{\text{sub}} \sim \mathcal{M}$  and compute  $1/|S_{\text{sub}}| \sum_{j \in S_{\text{sub}}} s_j(i)$  for  $i \in \bar{\mathcal{M}} \cup B_n$ . Then, we replace samples in  $\bar{\mathcal{M}}$  having smaller average KNN-SVs than samples in  $B_n$  with the input batch samples. ASER using both SV-based update and retrieval performs competitively or better than variations with just a random update or random retrieval (both random retrieval and update reduces to ER). This underscores the importance of SV-based methods for both *MemoryUpdate* and *MemoryRetrieval*. We use the KNN-SV *MemoryUpdate* throughout experiments in Section 5, and present ablation analysis of different variations in Appendix C.

## 5 Experiment

To test the efficacy of ASER and its variant  $\text{ASER}_\mu$ , we evaluate their performance by comparing them with several state-of-the-art CL baselines. We begin by reviewing the benchmark datasets, baselines we compared against and our experiment setting. We then report and analyze the result to validate our approach.

### 5.1 Datasets

**Split CIFAR-10** splits the CIFAR-10 dataset [15] into 5 different tasks with non-overlapping classes and 2 classes in each task, similarly as in [1].

**Split CIFAR-100** is constructed by splitting the CIFAR-100 dataset [15] into 10 disjoint tasks, and each task has 10 classes.

**Split miniImagenet** consists of splitting the miniImageNet dataset [32] into 10 disjoint tasks, where each task contains 10 classes

The detail of datasets, including the general information of each dataset, class composition and the number of samples in training, validation and test sets of each task is presented in Appendix E.

## 5.2 Baselines

We compare our proposed ASER against several state-of-the-art continual learning algorithms:

- **ASER & ASER $_{\mu}$** : Our proposed methods. ASER scores samples in the memory with **ASV** in (5). ASER $_{\mu}$  uses the mean variation **ASV $_{\mu}$**  in (6).
- **ER** [6]: Experience replay, a recent and successful rehearsal method with random sampling in *MemoryRetrieval* and reservoir sampling in *MemoryUpdate*.
- **GSS** [3]: Gradient-Based Sample Selection, a *MemoryUpdate* method that diversifies the gradients of the samples in the replay memory.
- **MIR** [1]: Maximally Interfered Retrieval, a *MemoryRetrieval* method that retrieves memory samples that suffer from an increase in loss given the estimated parameters update based on the current task.
- **iid-online & iid-offline**: iid-online trains the model with a single-pass through the same set of data, but each mini-batch is sampled iid from the training set. iid-offline trains the model over multiple epochs on the dataset with iid sampled mini-batch. We use 5 epochs for iid-offline in all the experiments as in [1, 3].
- **fine-tune**: As an important baseline in previous work [1, 3, 16], it simply trains the model in the order the data is presented without any specific method for forgetting avoidance.

We focus on ER-based methods for comparison since recent research has demonstrated the shortcomings of prior-focused methods in the task-free setting [18, 9], and [1] has shown ER-based methods outperform other memory-based methods. In Appendix D, we empirically verify this claim above by comparing ASER and ASER $_{\mu}$  to a variety of prior-focused and memory-based methods.

## 5.3 Experiment Setting

**Single-head Evaluation** Most of the previous work in CL applied multi-head evaluation [4] where a distinct output head is assigned for each task and the model utilizes the task metadata to choose the corresponding output head during test time. But in many realistic scenarios, task metadata is not available during test time, so the model should be able to classify labels from different tasks. As in [1, 3], we adopt the single-head evaluation setup where the model has one output head for all tasks and is required to classify all labels. Note that the setting we use – online and single-head evaluation – is more challenging than many other reported CL settings.

**Model** We use a reduced ResNet18, similar to [6, 20], as the base model for all datasets, and the network is trained via cross-entropy loss with SGD optimizer and mini-batch size of 10. The size of the mini-batch retrieved from memory is also set to 10 irrespective of the size of the memory.

## 5.4 Comparative Performance Evaluation

Table 1 and Table 2 show the average accuracy and average forgetting by the end of the data stream for Mini-ImageNet, CIFAR-100 and CIFAR-10. Based on the performance of iid-online and iid-offline, we verify that Mini-ImageNet and CIFAR-100 are more complex than CIFAR-10, even though three datasets have the same number of samples. Overall, ASER and ASER $_{\mu}$  show competitive or improved performance in three standard CL datasets. Especially, we observe that ASER $_{\mu}$  outperforms all the state-of-the-art baselines by significant margins in a more difficult setting where memory size is small and dataset is complex. Since the difficulty of the three datasets is different, comparing the absolute

Method	M=1k	M=2k	M=5k	M=1k	M=2k	M=5k	M=0.2k	M=0.5k	M=1k
iid online	14.7 ± 0.6	14.7 ± 0.6	14.7 ± 0.6	20.5 ± 0.4	20.5 ± 0.4	20.5 ± 0.4	62.9 ± 1.5	62.9 ± 1.5	62.9 ± 1.5
iid offline	42.4 ± 0.4	42.4 ± 0.4	42.4 ± 0.4	47.4 ± 0.3	47.4 ± 0.3	47.4 ± 0.3	79.7 ± 0.4	79.7 ± 0.4	79.7 ± 0.4
ER	8.7 ± 0.4	11.8 ± 0.9	16.5 ± 0.9	11.2 ± 0.4	14.6 ± 0.4	20.1 ± 0.8	26.4 ± 1.0	32.2 ± 1.4	38.4 ± 1.7
fine-tune	4.3 ± 0.2	4.3 ± 0.2	4.3 ± 0.2	5.9 ± 0.2	5.9 ± 0.2	5.9 ± 0.2	17.9 ± 0.4	17.9 ± 0.4	17.9 ± 0.4
GSS	7.5 ± 0.5	10.7 ± 0.8	12.5 ± 0.4	9.3 ± 0.2	10.9 ± 0.3	15.9 ± 0.4	26.9 ± 1.2	30.7 ± 1.2	40.1 ± 1.4
MIR	8.1 ± 0.3	11.2 ± 0.7	15.9 ± 1.6	11.2 ± 0.3	14.1 ± 0.2	21.2 ± 0.6	28.3 ± 1.6	35.6 ± 1.2	42.4 ± 1.5
ASER	<b>11.7 ± 0.7</b>	<b>14.4 ± 0.4</b>	<b>18.2 ± 0.7</b>	12.3 ± 0.4	14.7 ± 0.7	20.0 ± 0.6	27.8 ± 1.0	36.2 ± 1.1	43.1 ± 1.2
ASER <sub>μ</sub>	<b>12.2 ± 0.8</b>	<b>14.8 ± 1.1</b>	<b>18.2 ± 1.1</b>	<b>14.0 ± 0.4</b>	<b>17.2 ± 0.5</b>	21.7 ± 0.5	26.4 ± 1.5	36.3 ± 1.2	43.5 ± 1.4

(a) Mini-ImageNet

(b) CIFAR-100

(c) CIFAR-10

Table 1: Average Accuracy (higher is better), M is the memory buffer size. All numbers are the average of 15 runs. ASER<sub>μ</sub> has better performance when M is small and dataset is more complex.

Method	M=1k	M=2k	M=5k	M=1k	M=2k	M=5k	M=0.2k	M=0.5k	M=1k
ER	29.7 ± 1.3	29.2 ± 0.9	26.6 ± 1.1	45.0 ± 0.5	40.5 ± 0.8	34.5 ± 0.8	72.8 ± 1.7	63.1 ± 2.4	55.8 ± 2.6
fine-tune	35.6 ± 0.9	35.6 ± 0.9	35.6 ± 0.9	50.4 ± 1.0	50.4 ± 1.0	50.4 ± 1.0	81.7 ± 0.7	81.7 ± 0.7	81.7 ± 0.7
GSS	29.6 ± 1.2	27.4 ± 1.1	29.9 ± 1.2	46.9 ± 0.7	42.3 ± 0.8	39.2 ± 0.9	75.5 ± 1.5	65.9 ± 1.6	54.9 ± 2.0
MIR	29.7 ± 1.0	27.2 ± 1.1	26.2 ± 1.4	45.5 ± 0.8	40.4 ± 0.6	31.4 ± 0.6	67.0 ± 2.6	68.9 ± 1.7	47.7 ± 2.9
ASER	30.1 ± 1.3	<b>24.7 ± 1.0</b>	<b>20.9 ± 1.2</b>	50.1 ± 0.6	45.9 ± 0.9	36.7 ± 0.8	71.1 ± 1.8	<b>59.1 ± 1.5</b>	50.4 ± 1.5
ASER <sub>μ</sub>	28.0 ± 1.3	<b>22.2 ± 1.6</b>	<b>17.2 ± 1.4</b>	45.0 ± 0.7	<b>38.6 ± 0.6</b>	30.3 ± 0.5	72.4 ± 1.9	<b>58.8 ± 1.4</b>	47.9 ± 1.6

(a) Mini-ImageNet

(b) CIFAR-100

(c) CIFAR-10

Table 2: Average Forgetting (lower is better). Memory buffer size is M. All numbers are the average of 15 runs.

accuracy improvement may not be fair. Therefore, percentage improvement<sup>2</sup> is more appropriate here. Taking Mini-ImageNet as an example, ASER<sub>μ</sub> improves the strongest baseline by 40.2% (M=10), 25.4% (M=20) and 10.3% (M=50) in terms of percentage improvement. Moreover, as we can see in Figure 2, ASER<sub>μ</sub> is consistently better than other baselines in both datasets. We also note that ASER<sub>μ</sub> generally performs better than ASER. This is because if we use the ASV criterion as in (5), it has a higher chance that the value is affected by an outlier point in the *evaluation* set. So the ASV<sub>μ</sub> in (6) gives a more stable and accurate value in complicated datasets.

Another interesting observation is that ER has very competitive performances. Especially in more complex datasets, it surpasses GSS and performs similarly as MIR, which proves it to be a simple but powerful CL baseline. In addition, we find that for complex datasets, when memory size is larger than 5000 (10% of the training data), most of the replay-based methods (except for GSS) outperform the iid-online, a baseline that trains the model with a one-pass through the data but with iid-sampled mini-batch from the whole dataset. This means that storing a small number of training samples is crucial for combating forgetting as well as the learning of the current task in the task-free setting.

Overall, by evaluating on three standard CL datasets and comparing to the state-of-the-art CL methods, we have shown the effectiveness of ASER and its variant ASER<sub>μ</sub> in overcoming catastrophic forgetting, especially in more complex datasets and memory size is relatively small.

## 6 Conclusion

In this work, we proposed a novel ASER method that scores memory data samples according to their ability to preserve latent decision boundaries for previously observed classes while interfering with latent decision boundaries of current classes being learned. Overall, in the task-free CL setting, we observed that ASER and its ASER<sub>μ</sub> variant provide competitive or improved performance on a variety of datasets compared to state-of-the-art ER-based continual learning methods. We also remark that this work paves the way for a number of interesting research directions building on this work. Although our SV-based method has greatly improved the memory retrieval and update strategies,

<sup>2</sup>Percentage improvement is  $\frac{\text{absolute improvement}}{\text{baseline performance}}$ . For example, in Mini-ImageNet, when M=10, ASER<sub>μ</sub> improves MIR by  $\frac{12.2-8.7}{8.7} = 40.2\%$



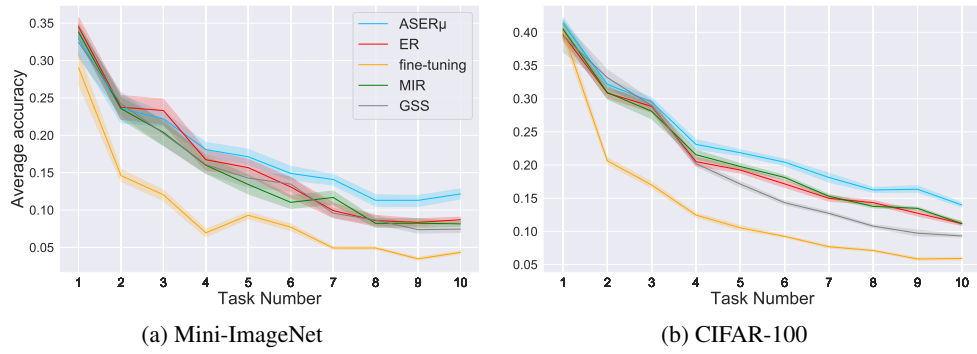


Figure 2: Average accuracy on observed tasks,  $M=1k$ . ASER $\mu$  outperforms other baselines especially when the model sees more classes (each task contains new classes)

we may be able to do better than simply concatenating retrieved samples with the incoming batch. Hence, future work could focus on more sophisticated methods to utilize the retrieved samples. It would also be interesting to investigate alternate CL-specific utility function variations for SV.

## Broader Impact

Continual learning (CL) is a critical problem to be addressed when considering deployed, online learning systems in practice that cannot store all data or repeatedly retrain from scratch. This is especially important when considering personal devices such as cell phones where CL may be required on-device to maintain privacy as well as real-time learning and adaptation capabilities. Furthermore, it is likely that no task metadata is given in these settings. In that regard, this work presents a novel state-of-the-art method for CL that works especially well in the low memory task-free setting. However, due to the extremely hard problem setting, we observe that the final performances of all considered models are quite low in more challenging datasets like CIFAR-100 and MiniImageNet. This implies that we still have a large room for improvement to deploy task-free CL methods in practice; nonetheless, we believe that this paper makes a positive forward step in the CL literature.

## References

- [1] Rahaf Aljundi, Eugene Belilovsky, Tinne Tuytelaars, Laurent Charlin, Massimo Caccia, Min Lin, and Lucas Page-Caccia. “Online Continual Learning with Maximal Interfered Retrieval”. In: *Advances in Neural Information Processing Systems 32*. 2019, pp. 11849–11860.
- [2] Rahaf Aljundi, Klaas Kelchtermans, and Tinne Tuytelaars. “Task-Free Continual Learning”. In: *The IEEE Conference on Computer Vision and Pattern Recognition (CVPR)*. June 2019.
- [3] Rahaf Aljundi, Min Lin, Baptiste Goujaud, and Yoshua Bengio. “Gradient based sample selection for online continual learning”. In: *Advances in Neural Information Processing Systems 32*. 2019, pp. 11816–11825.
- [4] Arslan Chaudhry, Puneet K Dokania, Thalaiyasingam Ajanthan, and Philip HS Torr. “Riemannian walk for incremental learning: Understanding forgetting and intransigence”. In: *Proceedings of the European Conference on Computer Vision (ECCV)*. 2018, pp. 532–547.
- [5] Arslan Chaudhry, Marc Aurelio Ranzato, Marcus Rohrbach, and Mohamed Elhoseiny. “Efficient Lifelong Learning with A-GEM”. In: *International Conference on Learning Representations*. 2019.
- [6] Arslan Chaudhry, Marcus Rohrbach, Mohamed Elhoseiny, Thalaiyasingam Ajanthan, Puneet K. Dokania, Philip H. S. Torr, and Marc Aurelio Ranzato. *On Tiny Episodic Memories in Continual Learning*. 2019. arXiv: 1902.10486 [cs.LG].
- [7] Matthias De Lange, Rahaf Aljundi, Marc Masana, Sarah Parisot, Xu Jia, Ales Leonardis, Gregory Slabaugh, and Tinne Tuytelaars. “Continual learning: A comparative study on how to defy forgetting in classification tasks”. In: *arXiv preprint arXiv:1909.08383* (2019).
- [8] Jeff Donahue, Yangqing Jia, Oriol Vinyals, Judy Hoffman, Ning Zhang, Eric Tzeng, and Trevor Darrell. “DeCAF: A Deep Convolutional Activation Feature for Generic Visual Recognition”. In: *Proceedings of the 31st International Conference on International Conference on Machine Learning - Volume 32*. ICML’14. JMLR.org, 2014, 1–647–1–655.
- [9] Sebastian Farquhar and Yarin Gal. *Towards Robust Evaluations of Continual Learning*. 2018. arXiv: 1805.09733 [stat.ML].
- [10] Jakob Foerster, Nantas Nardelli, Gregory Farquhar, Triantafyllos Afouras, Philip HS Torr, Pushmeet Kohli, and Shimon Whiteson. “Stabilising experience replay for deep multi-agent reinforcement learning”. In: *Proceedings of the 34th International Conference on Machine Learning - Volume 70*. JMLR. org. 2017, pp. 1146–1155.
- [11] Amirata Ghorbani and James Zou. “Data Shapley: Equitable Valuation of Data for Machine Learning”. In: *Proceedings of the 36th International Conference on Machine Learning*. Vol. 97. Proceedings of Machine Learning Research. PMLR, 2019, pp. 2242–2251.
- [12] Ruoxi Jia, David Dao, Boxin Wang, Frances Ann Hubis, Nezihe Merve Gurel, Bo Li, Ce Zhang, Costas Spanos, and Dawn Song. “Efficient Task-Specific Data Valuation for Nearest Neighbor Algorithms”. In: *Proc. VLDB Endow.* 12.11 (July 2019), pp. 1610–1623. ISSN: 2150-8097. DOI: 10.14778/3342263.3342637.
- [13] Ruoxi Jia, David Dao, Boxin Wang, Frances Ann Hubis, Nick Hynes, Nezihe Merve Gürel, Bo Li, Ce Zhang, Dawn Song, and Costas J. Spanos. “Towards Efficient Data Valuation Based on the Shapley Value”. In: *Proceedings of Machine Learning Research*. Vol. 89. Proceedings of Machine Learning Research. PMLR, 2019, pp. 1167–1176.

- [14] James Kirkpatrick, Razvan Pascanu, Neil Rabinowitz, Joel Veness, Guillaume Desjardins, Andrei A Rusu, Kieran Milan, John Quan, Tiago Ramalho, Agnieszka Grabska-Barwinska, et al. “Overcoming catastrophic forgetting in neural networks”. In: *Proceedings of the National Academy of Sciences of the United States of America* 114 13 (2017), pp. 3521–3526.
- [15] Alex Krizhevsky. *Learning Multiple Layers of Features from Tiny Images*. Tech. rep. University of Toronto, Apr. 2009.
- [16] Soochan Lee, Junsoo Ha, Dongsu Zhang, and Gunhee Kim. “A Neural Dirichlet Process Mixture Model for Task-Free Continual Learning”. In: *International Conference on Learning Representations*. 2020.
- [17] Timothée Lesort, Hugo Caselles-Dupré, Michaël Garcia Ortiz, Andrei Stoian, and David Filliat. *Generative Models from the perspective of Continual Learning*. 2018. arXiv: 1812.09111 [cs.LG].
- [18] Timothée Lesort, Andrei Stoian, and David Filliat. “Regularization Shortcomings for Continual Learning”. In: *arXiv preprint arXiv:1912.03049* (2019).
- [19] Zhizhong Li and Derek Hoiem. “Learning Without Forgetting”. In: *ECCV*. Springer. 2016, pp. 614–629.
- [20] David Lopez-Paz and Marc’Aurelio Ranzato. “Gradient Episodic Memory for Continual Learning”. In: *Advances in Neural Information Processing Systems 30*. 2017, pp. 6467–6476.
- [21] Laurens van der Maaten and Geoffrey Hinton. “Visualizing Data using t-SNE”. In: *Journal of Machine Learning Research* 9 (2008), pp. 2579–2605.
- [22] Arun Mallya and Svetlana Lazebnik. “Packnet: Adding multiple tasks to a single network by iterative pruning”. In: *Proceedings of the IEEE Conference on Computer Vision and Pattern Recognition*. 2018, pp. 7765–7773.
- [23] Michael McCloskey and Neal J Cohen. “Catastrophic interference in connectionist networks: The sequential learning problem”. In: *Psychology of learning and motivation*. Vol. 24. Elsevier, 1989, pp. 109–165.
- [24] Renqiang Min, David A. Stanley, Zineng Yuan, Anthony Bonner, and Zhaolei Zhang. “A Deep Non-Linear Feature Mapping for Large-Margin KNN Classification”. In: *Proceedings of the 2009 Ninth IEEE International Conference on Data Mining. ICDM ’09*. IEEE Computer Society, 2009, pp. 357–366. DOI: 10.1109/ICDM.2009.27.
- [25] Cuong V. Nguyen, Yingzhen Li, Thang D. Bui, and Richard E. Turner. “Variational Continual Learning”. In: *International Conference on Learning Representations*. 2018.
- [26] German I. Parisi, Ronald Kemker, Jose L. Part, Christopher Kanan, and Stefan Wermter. “Continual lifelong learning with neural networks: A review”. In: *Neural Networks* 113 (2019), pp. 54–71.
- [27] Matthew Reimer, Ignacio Cases, Robert Ajemian, Miao Liu, Irina Rish, Yuhai Tu, and Gerald Tesauro. “Learning to Learn without Forgetting by Maximizing Transfer and Minimizing Interference”. In: *ICLR*. 2019.
- [28] David Rolnick, Arun Ahuja, Jonathan Schwarz, Timothy Lillicrap, and Gregory Wayne. “Experience replay for continual learning”. In: *Advances in Neural Information Processing Systems*. 2019, pp. 348–358.
- [29] Alvin E Roth. *The Shapley value: essays in honor of Lloyd S. Shapley*. Cambridge University Press, 1988.
- [30] Lloyd S Shapley. “A value for n-person games”. In: *Contributions to the Theory of Games* 2.28 (1953), pp. 307–317.
- [31] Hanul Shin, Jung Kwon Lee, Jaehong Kim, and Jiwon Kim. “Continual learning with deep generative replay”. In: *Advances in Neural Information Processing Systems*. 2017, pp. 2990–2999.
- [32] Oriol Vinyals, Charles Blundell, Timothy Lillicrap, koray kavukcuoglu koray, and Daan Wierstra. “Matching Networks for One Shot Learning”. In: *Advances in Neural Information Processing Systems 29*. 2016, pp. 3630–3638.
- [33] Jaehong Yoon, Eunho Yang, Jeongtae Lee, and Sung Ju Hwang. “Lifelong Learning with Dynamically Expandable Networks”. In: *International Conference on Learning Representations*. 2018. URL: <https://openreview.net/forum?id=Sk7KsfW0->.

- [34] Friedemann Zenke, Ben Poole, and Surya Ganguli. “Continual learning through synaptic intelligence”. In: *Proceedings of the 34th International Conference on Machine Learning-Volume 70*. JMLR. org. 2017, pp. 3987–3995.

## Appendix

### A Detail of Experiments

We use a reduced ResNet18, similar to [6, 20], as the base model for all datasets, and the network is trained via cross-entropy loss with SGD optimizer. For all experiments, we use a learning rate of 0.1. The mini-batch size is 10 and the size of the mini-batch retrieved from memory is also set to 10 irrespective of the size of the memory. Since we apply the online setting, the model only sees each batch once, so the number of epochs is set to 1 for all experiments.

The code to reproduce all results can be found in the attached zip file.

### B Properties of KNN Shapley Value

We prove the properties of KNN-SV presented in Section 4. Given a candidate sample  $i = (\mathbf{x}_i, y_i) \in D_c$  and an evaluation point  $j = (\mathbf{x}_j^{\text{ev}}, y_j^{\text{ev}})$ , where  $D_c$  is a candidate set with  $|D_c| = N_c$ , we denote the KNN-SV of the point  $i$  w.r.t. the evaluation point  $j$  as  $s_j(i)$ . For notational convenience, we assume that points in  $D_c$  are sorted based on distances from the evaluation point in ascending order. In other words,  $d(i, j) \leq d(i', j) \forall i < i'$  where  $d(i, j)$  is the distance between  $\mathbf{x}_i$  and  $\mathbf{x}_j^{\text{ev}}$ .

**Property 1.**  $s_j(i) > 0$  if and only if  $y_i = y_j^{\text{ev}}$ . Also,  $s_j(i) = 0$  only when  $S = \{i' | y_{i'} = y_j^{\text{ev}}, \forall i' \in \{i + 1, \dots, N_c\}\} = \emptyset$ .

*Proof.* Firstly, we prove  $s_j(i) > 0$  if and only if  $y_i = y_j^{\text{ev}}$  along with another statement,  $|s_j(i)| < \frac{1}{i-1}$ . The proof is by induction, starting from the base case when  $i = N_c$ . When  $i = N_c$ ,  $s_j(N_c) = \frac{\mathbb{1}(y_{N_c} = y_j^{\text{ev}})}{N_c}$  as per (3). Hence,  $s_j(N_c) > 0$  holds iff  $y_{N_c} = y_j^{\text{ev}}$ . Additionally, we see that  $|s_j(N_c)| \leq \frac{1}{N_c} < \frac{1}{N_c-1}$ . We can also verify the case for  $i = N_c - 1$  using (4):

$$s_j(N_c - 1) = \begin{cases} \frac{1}{N_c} > 0 & \text{if } y_{N_c-1} = y_{N_c} = y_j^{\text{ev}} \\ \frac{1}{N_c-1} > 0 & \text{if } y_{N_c-1} = y_j^{\text{ev}} \neq y_{N_c} \\ \frac{1}{N_c} - \frac{1}{N_c-1} < 0 & \text{if } y_{N_c-1} \neq y_j^{\text{ev}} \ \& \ y_{N_c} = y_j^{\text{ev}} \\ 0 & \text{if } y_{N_c-1} \neq y_j^{\text{ev}} \ \& \ y_{N_c} \neq y_j^{\text{ev}} \end{cases} \quad (\text{B.1})$$

So, we again note that  $s_j(N_c - 1) > 0$  iff  $y_{N_c-1} = y_j^{\text{ev}}$ , and  $|s_j(N_c - 1)| \leq \frac{1}{N_c-1} < \frac{1}{N_c-2}$  holds.

Now, assume for  $i = m \geq K + 1$ ,  $s_j(m) > 0$  iff  $y_m = y_j^{\text{ev}}$  and  $|s_j(m)| < \frac{1}{m-1}$ . Then, for  $i = m - 1 \geq K$ ,

$$\begin{aligned} s_j(m-1) &= s_j(m) + \frac{\mathbb{1}(y_{m-1} = y_j^{\text{ev}}) - \mathbb{1}(y_m = y_j^{\text{ev}})}{m-1} \\ &= \begin{cases} s_j(m) > 0 & \text{if } y_{m-1} = y_m = y_j^{\text{ev}}, \\ s_j(m) + \frac{1}{m-1} > 0 & \text{if } y_{m-1} = y_j^{\text{ev}} \neq y_m, \\ s_j(m) - \frac{1}{m-1} < 0 & \text{if } y_{m-1} \neq y_j^{\text{ev}} \ \& \ y_m = y_j^{\text{ev}}, \\ s_j(m) \leq 0 & \text{if } y_{m-1} \neq y_j^{\text{ev}} \ \& \ y_m \neq y_j^{\text{ev}}. \end{cases} \quad (\text{B.2}) \end{aligned}$$

Note that the second and the third cases in (B.2) hold because  $|s_j(m)| < \frac{1}{m-1}$  by assumption. Additionally, it is straightforward to check that  $|s_j(m-1)| < \frac{1}{m-2}$  holds for all cases. Hence, we have shown the statement holds for  $m \geq K$ .

For  $m < K$ , we firstly note that  $|s_j(K)| \leq 1/K$  because  $|s_j(K+1)| < 1/K$  and  $s_j(K) = s_j(K+1) + \frac{\mathbb{1}(y_K = y_j^{\text{ev}}) - \mathbb{1}(y_{K+1} = y_j^{\text{ev}})}{K}$ . Then, we see that the increment and the decrement, if any, are always  $\frac{1}{K}$  for  $m < K$ . Therefore,  $s_j(m) > 0$  iff  $y_m = y_j^{\text{ev}}$ . Furthermore, we have noted that the sign of  $s_j(i)$  has to change iff  $\mathbb{1}(y_i = y_j^{\text{ev}}) \neq \mathbb{1}(y_{i+1} = y_j^{\text{ev}})$  because  $|s_j(i+1)| < 1/i$ . This implies  $s_j(i) = 0$  only when  $S = \{i' | y_{i'} = y_j^{\text{ev}}, \forall i' \in \{i+1, \dots, N_c\}\} = \emptyset$ , and we conclude the proof.  $\square$

**Property 2.**  $|s_j(m)|$  is a non-increasing function of  $m$  for  $m$  such that  $y_m = y_j^{\text{ev}}$ . Similarly,  $|s_j(n)|$  is a non-increasing function of  $n$  for  $n$  such that  $y_n \neq y_j^{\text{ev}}$ . And for  $m \geq K$ ,  $|s_j(m)| - |s_j(m')| > 0$  holds for  $m < m'$ , where  $m'$  is the smallest index with  $\mathbb{1}(y_m = y_j^{\text{ev}}) = \mathbb{1}(y_{m'} = y_j^{\text{ev}})$ , if there exists  $l \in (m, m')$  such that  $\mathbb{1}(y_l = y_j^{\text{ev}}) \neq \mathbb{1}(y_m = y_j^{\text{ev}})$ . In other words, as  $i$  gets closer to the evaluation point  $j$ ,  $|s_j(i)|$  cannot decrease for points with the same  $\mathbb{1}(y_i = y_j^{\text{ev}})$ , and for  $i \geq K$ , it can only increase when there exist more than one differently labeled points.

*Proof.* We only show for  $m$  such that  $y_m = y_j^{\text{ev}}$  as it can be similarly done for  $n$  with  $y_n \neq y_j^{\text{ev}}$ . If  $y_l = y_j^{\text{ev}} \forall l \in (m, m']$ , then it trivially holds that  $s_j(m) = s_j(m')$ . Now, assume that there exists one  $l \in (m, m')$  such that  $y_l \neq y_j^{\text{ev}}$  and that  $l = m + 1$ . Then, we see that  $|s_j(m)| - |s_j(m')| > 0$  holds. This is because

$$\begin{aligned}
s_j(m) &= s_j(m+1) + \frac{\mathbb{1}(y_m = y_j^{\text{ev}}) - \mathbb{1}(y_{m+1} = y_j^{\text{ev}})}{m} \\
&= s_j(m+2) + \frac{\mathbb{1}(y_{m+1} = y_j^{\text{ev}}) - \mathbb{1}(y_{m+2} = y_j^{\text{ev}})}{m+1} + \frac{1}{m} \\
&= s_j(m+2) - \frac{1}{m+1} + \frac{1}{m} \\
&= s_j(m+2) + \left(\frac{1}{m} - \frac{1}{m+1}\right) > s_j(m+2) = s_j(m'), \quad \forall m' \geq m+2 \quad (\text{B.3})
\end{aligned}$$

Then, we note that  $s_j(m'') = s_j(m)$  for all  $m'' \in (i, m]$  where  $i < m$  is the largest index with  $y_i \neq y_j^{\text{ev}}$  (if exists) or  $i = 0$ . This shows that  $|s_j(m)| > |s_j(m')|$  holds for  $m < m'$  if there is a single  $l \in (m, m')$  with  $y_l \neq y_j^{\text{ev}}$ . When there are multiple (possibly consecutive) points with  $y_l \neq y_j^{\text{ev}}$ , we can always select  $\hat{m} \geq m$  such that there is only a single point (or several consecutive points)  $l$  with  $y_l \neq y_j^{\text{ev}}$ , leading to  $|s_j(\hat{m})| > |s_j(m')|$ . By applying this multiple times, we get  $|s_j(m)| > |s_j(m')|$ .  $\square$

## C Ablation Studies

In ASER & ASER $_{\mu}$ , we use ASV and ASV $_{\mu}$  for scoring samples for *MemoryRetrieval*, while KNN-SV is used for scoring samples for *MemoryUpdate*. In this part, we examine several ablations to understand contributions of each component in ASER methods. In addition to ASER, ASER $_{\mu}$  and ER as in Section 5, we compare 3 more variations:

- **SV-upd:** Use KNN-SV *MemoryUpdate* as described in Section 4 while randomly retrieving samples from the memory for replay.
- **ASV-ret:** Use (5) scoring function for *MemoryRetrieval* while using reservoir sampling for *MemoryUpdate*.
- **ASV $_{\mu}$ -ret:** Use (6) scoring function for *MemoryRetrieval* while using reservoir sampling for *MemoryUpdate*.

Table C.1 compares the average accuracy of these variations. As for CIFAR-10, we can see that all SV-based methods improve upon ER. In particular, ASER and ASER $_{\mu}$  show the largest improvements, suggesting the effectiveness of the combination of the KNN-SV based *MemoryRetrieval* and *MemoryUpdate*. For the other two datasets, it turns out that SV-upd is a powerful *MemoryUpdate* method. Compared to GSS [3] which suggests another *MemoryUpdate* method, we observe significant performance boosts (see Table 1). In these two datasets, ASV $_{\mu}$ -ret methods and ER perform comparably. However, we note that we can further fight the forgetting when *MemoryRetrieval* and *MemoryUpdate* are used together (Table C.2). In summary, ASER using both SV-based update and retrieval performs competitively or better than variations with just a random update or random retrieval (both random retrieval and update reduce to ER). This underscores the importance of SV-based methods for both *MemoryUpdate* and *MemoryRetrieval*.

Method	M=1k	M=2k	M=5k	M=1k	M=2k	M=5k	M=0.2k	M=0.5k	M=1k
ER	8.7 ± 0.4	11.8 ± 0.9	16.5 ± 0.9	11.2 ± 0.4	14.6 ± 0.4	20.1 ± 0.8	26.4 ± 1.0	32.2 ± 1.4	38.4 ± 1.7
SV-upd	<b>13.4 ± 0.8</b>	<b>15.5 ± 0.7</b>	<b>18.4 ± 0.4</b>	<b>14.0 ± 0.6</b>	<b>17.2 ± 0.4</b>	20.9 ± 0.6	25.9 ± 0.6	33.7 ± 1.4	41.2 ± 1.3
ASV-ret	6.9 ± 0.4	9.9 ± 0.9	16.2 ± 0.8	10.1 ± 0.3	13.9 ± 0.3	20.3 ± 0.3	26.6 ± 1.0	34.7 ± 1.1	39.3 ± 1.6
ASV <sub>μ</sub> -ret	7.4 ± 0.6	10.0 ± 1.0	17.1 ± 0.9	10.8 ± 0.3	14.8 ± 0.4	<b>21.7 ± 0.3</b>	25.8 ± 1.0	35.7 ± 1.4	40.2 ± 1.0
ASER	11.7 ± 0.8	14.4 ± 0.4	<b>18.2 ± 0.7</b>	12.3 ± 0.4	14.7 ± 0.7	20.0 ± 0.6	<b>27.8 ± 1.0</b>	36.2 ± 1.1	<b>43.1 ± 1.2</b>
ASER <sub>μ</sub>	12.2 ± 0.8	<b>14.8 ± 1.1</b>	<b>18.2 ± 1.1</b>	<b>14.0 ± 0.4</b>	<b>17.2 ± 0.5</b>	<b>21.7 ± 0.5</b>	26.4 ± 1.5	36.3 ± 1.2	<b>43.5 ± 1.4</b>

(a) Mini-ImageNet

(b) CIFAR-100

(c) CIFAR-10

Table C.1: Ablation analysis. Average Accuracy (higher is better). Memory buffer size M.

Method	M=1k	M=2k	M=5k	M=1k	M=2k	M=5k	M=0.2k	M=0.5k	M=1k
ER	29.7 ± 1.3	29.2 ± 0.9	26.6 ± 1.1	45.5 ± 0.5	40.5 ± 0.8	34.5 ± 0.8	72.8 ± 1.7	63.1 ± 2.4	55.8 ± 2.6
SV-upd	29.2 ± 1.1	26.4 ± 1.5	24.6 ± 1.3	45.9 ± 0.7	41.6 ± 0.7	36.6 ± 0.5	73.6 ± 1.0	63.4 ± 1.6	52.4 ± 2.0
ASV-ret	<b>27.6 ± 1.2</b>	27.7 ± 1.3	25.5 ± 1.2	47.4 ± 0.4	42.0 ± 0.6	34.5 ± 0.8	71.7 ± 2.1	60.1 ± 1.7	53.5 ± 2.5
ASV <sub>μ</sub> -ret	<b>28.3 ± 1.3</b>	27.4 ± 1.2	23.2 ± 1.6	45.5 ± 0.7	<b>37.4 ± 0.5</b>	31.8 ± 0.6	73.6 ± 1.4	58.3 ± 2.2	49.0 ± 2.2
ASER	30.1 ± 1.3	24.7 ± 1.0	20.9 ± 1.2	50.1 ± 0.6	45.9 ± 0.9	36.7 ± 0.8	71.1 ± 1.8	59.1 ± 1.5	50.4 ± 1.5
ASER <sub>μ</sub>	<b>28.0 ± 1.3</b>	<b>22.2 ± 1.6</b>	<b>17.2 ± 1.4</b>	45.0 ± 0.7	38.6 ± 0.6	<b>30.3 ± 0.5</b>	72.4 ± 1.9	58.8 ± 1.4	<b>47.9 ± 1.6</b>

(a) Mini-ImageNet

(b) CIFAR-100

(c) CIFAR-10

Table C.2: Ablation analysis. Average Forgetting (lower is better). Memory buffer size M.

## D Detailed Performance Evaluation

Following the definition of **ASV** and **ASV<sub>μ</sub>**, we can replace the Shapley value with distance (we use Euclidean as example) in (5) and (6). Specifically, we want to retrieve a point  $i$  such that its distances from samples of the same label in  $\mathcal{M}$  and its distances from input batch samples are both small. Concretely, the score for a candidate point  $i$  is defined as follows:

$$\mathbf{Dist}(i) = - \left[ \min_{j \in S_{\text{sub}}(i)} d(i, j) + \min_{k \in B_n} d(i, k) \right], \quad \forall i \in \mathcal{M} \setminus S_{\text{sub}}, \quad (\text{D.1})$$

as well as a “softer” mean variation **Dist<sub>μ</sub>**

$$\mathbf{Dist}_{\mu}(i) = - \left[ \frac{1}{|S_{\text{sub}}(i)|} \sum_{j \in S_{\text{sub}}(i)} d(i, j) + \frac{1}{b} \sum_{k \in B_n} d(i, k) \right], \quad \forall i \in \mathcal{M} \setminus S_{\text{sub}}. \quad (\text{D.2})$$

Here,  $S_{\text{sub}}$  is defined as in Section 4 and  $S_{\text{sub}}(i) = \{i' | i' \in S_{\text{sub}} \ \& \ y_{i'} = y_i\}$ .  $d(i, j)$  is the Euclidean distance between the candidate point  $i$  and an evaluation point  $j$  in the latent space. Finally, we simply replace the score in Algorithm 2 (line 9) with either one of the above scores.

### D.1 Detailed Result Tables

In addition to the algorithms listed in Section 5, in Table D.1 and Table D.2, we include more baselines for comparison:

- **AGEM** [5]: Averaged Gradient Episodic Memory, a memory-based method that utilizes the samples in the memory buffer to constrain the parameter updates.
- **ASER & ASER<sub>μ</sub>**: Our proposed methods. ASER scores samples in the memory with **ASV** in (5). ASER<sub>μ</sub> uses the mean variation **ASV<sub>μ</sub>** in (6).
- **Dist & Dist<sub>μ</sub>**: The Euclidean variants of ASER & ASER<sub>μ</sub> that replace Shapley value with Euclidean distance, as described above.
- **ER** [6]: Experience replay, a recent and successful rehearsal method with random sampling in *MemoryRetrieval* and reservoir sampling in *MemoryUpdate*.
- **EWC** [14]: Elastic Weight Consolidation, a prior-focused method that limits the update of parameters that were important to the past tasks, as measured by the Fisher information matrix.

Method	M=1k	M=2k	M=5k	M=1k	M=2k	M=5k	M=0.2k	M=0.5k	M=1k
iid online	14.7 ± 0.6	14.7 ± 0.6	14.7 ± 0.6	20.5 ± 0.4	20.5 ± 0.4	20.5 ± 0.4	62.9 ± 1.5	62.9 ± 1.5	62.9 ± 1.5
iid offline	42.4 ± 0.4	42.4 ± 0.4	42.4 ± 0.4	47.4 ± 0.3	47.4 ± 0.3	47.4 ± 0.3	79.7 ± 0.4	79.7 ± 0.4	79.7 ± 0.4
AGEM	7.0 ± 0.4	7.1 ± 0.5	6.9 ± 0.7	9.5 ± 0.4	9.3 ± 0.4	9.7 ± 0.3	22.7 ± 1.8	22.7 ± 1.9	22.6 ± 0.7
ER	8.7 ± 0.4	11.8 ± 0.9	16.5 ± 0.9	11.2 ± 0.4	14.6 ± 0.4	20.1 ± 0.8	26.4 ± 1.0	32.2 ± 1.4	38.4 ± 1.7
EWC	3.1 ± 0.3	3.1 ± 0.3	3.1 ± 0.3	4.8 ± 0.2	4.8 ± 0.2	4.8 ± 0.2	17.9 ± 0.3	17.9 ± 0.3	17.9 ± 0.3
fine-tune	4.3 ± 0.2	4.3 ± 0.2	4.3 ± 0.2	5.9 ± 0.2	5.9 ± 0.2	5.9 ± 0.2	17.9 ± 0.4	17.9 ± 0.4	17.9 ± 0.4
GSS	7.5 ± 0.5	10.7 ± 0.8	12.5 ± 0.4	9.3 ± 0.2	10.9 ± 0.3	15.9 ± 0.4	26.9 ± 1.2	30.7 ± 1.2	40.1 ± 1.4
MIR	8.1 ± 0.3	11.2 ± 0.7	15.9 ± 1.6	11.2 ± 0.3	14.1 ± 0.2	21.2 ± 0.6	28.3 ± 1.6	35.6 ± 1.2	42.4 ± 1.5
ASER	<b>11.7 ± 0.8</b>	<b>14.4 ± 0.4</b>	<b>18.2 ± 0.7</b>	12.3 ± 0.4	14.7 ± 0.7	20.0 ± 0.6	27.8 ± 1.0	36.2 ± 1.1	43.1 ± 1.2
ASER <sub>μ</sub>	<b>12.2 ± 0.8</b>	<b>14.8 ± 1.1</b>	<b>18.2 ± 1.1</b>	<b>14.0 ± 0.4</b>	<b>17.2 ± 0.5</b>	21.7 ± 0.5	26.4 ± 1.5	36.3 ± 1.2	43.5 ± 1.4
Dist	7.9 ± 0.5	10.4 ± 0.7	15.5 ± 0.9	10.3 ± .3	12.4 ± 0.5	16.7 ± 0.6	22.9 ± 0.9	31.6 ± 1.7	38.0 ± 2.3
Dist <sub>μ</sub>	8.1 ± 0.5	9.1 ± 0.7	14.9 ± 0.9	10.5 ± 0.2	13.4 ± 0.4	17.2 ± 0.8	23.4 ± 1.0	29.7 ± 1.2	35.6 ± 1.3

(a) Mini-ImageNet

(b) CIFAR-100

(c) CIFAR-10

Table D.1: Average Accuracy(higher is better). Memory buffer size M.

Method	M=1k	M=2k	M=5k	M=1k	M=2k	M=5k	M=0.2k	M=0.5k	M=1k
AGEM	29.3 ± 0.9	30.0 ± 0.9	29.9 ± 0.8	40.4 ± 0.7	39.7 ± 0.8	39.8 ± 1.0	36.1 ± 3.8	43.2 ± 4.2	48.1 ± 3.0
ER	29.7 ± 1.3	29.2 ± 0.9	26.6 ± 1.1	45.0 ± 0.5	40.5 ± 0.8	34.5 ± 0.8	72.8 ± 1.7	63.1 ± 2.4	55.8 ± 2.6
EWC	28.1 ± 0.8	28.1 ± 0.8	28.1 ± 0.8	39.1 ± 1.2	39.1 ± 1.2	39.1 ± 1.2	81.5 ± 1.4	81.5 ± 1.4	81.5 ± 1.4
fine-tune	35.6 ± 0.9	35.6 ± 0.9	35.6 ± 0.9	50.4 ± 1.0	50.4 ± 1.0	50.4 ± 1.0	81.7 ± 0.7	81.7 ± 0.7	81.7 ± 0.7
GSS	29.6 ± 1.2	27.4 ± 1.1	29.9 ± 1.2	46.9 ± 0.7	42.3 ± 0.8	39.2 ± 0.9	75.5 ± 1.5	65.9 ± 1.6	54.9 ± 2.0
MIR	29.7 ± 1.0	27.2 ± 1.1	26.2 ± 1.4	45.5 ± 0.8	40.4 ± 0.6	31.4 ± 0.6	<b>67.0 ± 2.6</b>	68.9 ± 1.7	<b>47.7 ± 2.9</b>
ASER	30.1 ± 1.3	24.7 ± 1.0	20.9 ± 1.2	50.1 ± 0.6	45.9 ± 0.9	36.7 ± 0.8	71.1 ± 1.8	59.1 ± 1.5	50.4 ± 1.5
ASER <sub>μ</sub>	28.0 ± 1.3	<b>22.2 ± 1.6</b>	<b>17.2 ± 1.4</b>	45.0 ± 0.7	<b>38.6 ± 0.6</b>	<b>30.3 ± 0.5</b>	72.4 ± 1.9	58.8 ± 1.4	47.9 ± 1.6
Dist	30.4 ± 1.1	25.5 ± 1.7	26.3 ± 1.2	48.1 ± 0.8	43.8 ± 0.5	39.5 ± 0.8	76.4 ± 2.3	<b>63.7 ± 2.3</b>	53.6 ± 3.8
Dist <sub>μ</sub>	29.7 ± 1.1	29.8 ± 1.1	27.1 ± 1.4	48.0 ± 0.6	43.5 ± 0.6	39.9 ± 0.8	77.6 ± 1.6	68.6 ± 2.0	58.8 ± 2.7

(a) Mini-ImageNet

(b) CIFAR-100

(c) CIFAR-10

Table D.2: Average Forgetting (lower is better). Memory buffer size M.

- **GSS** [3]: Gradient-Based Sample Selection, a *MemoryUpdate* method that diversifies the gradients of the samples in the replay memory.
- **MIR** [1]: Maximally Interfered Retrieval, a *MemoryRetrieval* method that retrieves memory samples that suffer from an increase in loss given the estimated parameters update based on the current task.
- **iid-online & iid-offline**: iid-online trains the model with a single-pass through the same set of data, but each mini-batch is sampled iid from the training set. iid-offline trains the model over multiple epochs on the dataset with iid sampled mini-batch. We use 5 epochs for iid-offline in all the experiments as in [1, 3].
- **fine-tune**: As an important baseline in previous work [1, 3, 16], it simply trains the model in the order the data is presented without any specific method for forgetting avoidance.

As we can see from Table D.1, Table D.2 and Figure D.1, ASER and ASER<sub>μ</sub> outperform Dist and Dist<sub>μ</sub>. The reason may be that both ASER methods do not greedily retrieve samples with the smallest distances to either  $S_{\text{sub}}$  (sub-sample from  $\mathcal{M}$ ) or  $B_n$  (incoming mini-batch). This is because for a single evaluation point  $j$ ,  $s_j(\alpha_m) = s_j(\alpha_{m+1})$  when  $y_{\alpha_m} = y_{\alpha_{m+1}}$ . So, a few points can have the same score even if some of them are farther from the evaluation point.

We also verify some claims from previous work [18, 9, 1]. EWC, a prior-focused method, not only is surpassed by all memory-based methods but also underperforms the fine-tuning baseline. Additionally, AGEM, a method that uses memory samples to constrain parameter updates, delivers worse performance compared with replay-based methods (ER, MIR, and GSS), especially when memory size increases.



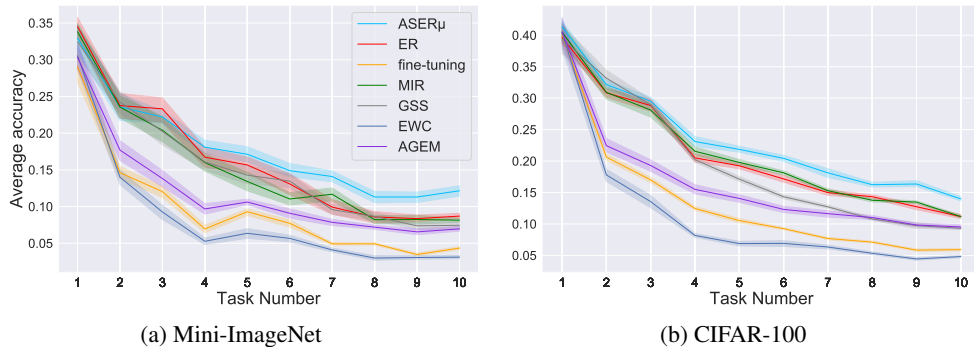


Figure D.1: Average accuracy on observed tasks,  $M=1k$ .  $ASER_{\mu}$  outperforms other baselines especially when the model sees more classes (each task contains new classes). In the task-free setting, EWC(no memory used) performs worse than memory-based methods.

	Split Mini-ImageNet	Split CIFAR-100	Split CIFAR-10
num. of tasks	10	10	5
image size	3x84x84	3x32x32	3x32x32
num. of classes per task	10	10	2
num. of training images per task	4800	4500	9000
num. of validation images per task	600	500	1000
num. of testing images per task	600	1000	1000

Table E.1: Dataset statistics

## E Dataset Detail

Table E.1 shows the summary of the datasets used for the experiments. For a fair comparison, the classes in each task and the order of tasks are fixed in all experiments. For Split CIFAR-10, the first task contains class [0, 1], the second task contains class [2, 3], and so on. For Split CIFAR-100, similar to Split CIFAR-10, the first task contains class [0, 1, ..., 9], the second task contains class [10, 11, ..., 19] and so on.

In original Mini-ImageNet, 100 classes are divided into 64, 16, and 20 classes respectively for meta-training, meta-validation, and meta-test [32]. For Split Mini-ImageNet, we firstly combine 64, 16, and 20 classes into one dataset. The first task contains the first 10 classes; the second task contains the next 10 classes, and so on.